Acta Biomaterialia 96 (2019) 310–320

Contents lists available at ScienceDirect

Acta Biomaterialia

journal homepage: www.elsevier.com/locate/actabiomat

Full length article

Extracellular matrix type modulates mechanotransduction of stem cells

Alice E. Stanton [a], Xinming Tong [b], Fan Yang [a,b,*]

[a] Department of Bioengineering, Stanford University, Stanford, CA 94305, USA
[b] Department of Orthopaedic Surgery, Stanford University, Stanford, CA 94305, USA

ARTICLE INFO

Article history:
Received 1 February 2019
Received in revised form 24 June 2019
Accepted 25 June 2019
Available online 28 June 2019

Keywords:
YAP
Mechanotransduction
Stem cells
Hydrogel
ECM

ABSTRACT

Extracellular matrix (ECM) is comprised of different types of proteins, which change in composition and ratios during morphogenesis and disease progression. ECM proteins provide cell adhesion and impart mechanical cues to the cells. Increasing substrate stiffness has been shown to induce Yes-associated protein (YAP) translocation from the cytoplasm to the nucleus, yet these mechanistic studies used fibronectin only as the biochemical cue. How varying the types of ECM modulates mechanotransduction of stem cells remains largely unknown. Using polyacrylamide hydrogels with tunable stiffness as substrates, here we conjugated four major ECM proteins commonly used for cell adhesion: fibronectin, collagen I, collagen IV and laminin, and assessed the effects of varying ECM type and density on YAP translocation in human mesenchymal stem cells (hMSCs). For all four ECM types, increasing ECM ligand density alone can induce YAP nuclear translocation without changing substrate stiffness. The ligand threshold for such biochemical ligand-induced YAP translocation differs across ECM types. While stiffness-dependent YAP translocation can be induced by all four ECM types, each ECM requires a different optimized ligand density for this to occur. Using antibody blocking, we further identified integrin subunits specifically involved in mechanotransduction of different ECM types. Finally, we demonstrated that altering ECM type further modulates hMSC osteogenesis without changing substrate stiffness. These findings highlight the important role of ECM type in modulating mechanotransduction and differentiation of stem cells, and call for future mechanistic studies to further elucidate the role of changes in ECM compositions in mediating mechanotransduction during morphogenesis and disease progression.

Statement of Significance

Our study addresses a critical gap of knowledge in mechanobiology. Increasing substrate stiffness has been shown to induce nuclear YAP translocation, yet only on fibronectin-coated substrates. However, extracellular matrix (ECM) is comprised of different protein types. How varying the type of ECM modulates stem cell mechanotransduction remains largely unknown.

We here reveal that the choice of ECM type can directly modulate stem cell mechanotransduction, filling this critical gap.

This work has broad impacts in mechanobiology and biomaterials, as it provides the first evidence that varying ECM type can impact YAP translocation independent of substrate stiffness, opening doors for a more rational biomaterials design tuning ECM properties to control cell fate for promoting normal development and for preventing disease progression.

1. Introduction

Stem cell behavior is altered by the mechanical and biochemical properties of the surrounding extracellular matrix (ECM) [1]. ECM support cell adhesion, among many other functions, and is comprised of over 300 proteins and 200 glycoproteins [2]. These adhesive proteins are sensed by integrin receptors on the cell membrane, which bind to the matrix and recruit focal adhesion

Abbreviations: YAP, Yes-associated protein; ECM, extracellular matrix; hMSC, human mesenchymal stem cell; BM, basement membrane; RUNX2, runt-related transcription factor 2; ALP, alkaline phosphatase.

* Corresponding author at: Departments of Bioengineering and Orthopaedic Surgery, Director of Stem Cells and Biomaterials Engineering Laboratory, Stanford University School of Medicine, 300 Pasteur Dr., Edwards R105, Stanford, CA 94305, USA.

E-mail address: fanyang@stanford.edu (F. Yang).

https://doi.org/10.1016/j.actbio.2019.06.048
1742-7061/

proteins and cytoskeletal elements to form stable adhesions that can transmit and transduce force [1]. Stiffer matrices lead to more stable adhesions and actin stress fibers that result in cell spreading [3] and translocation of the transcriptional regulator Yes-associated protein (YAP) from the cytoplasm to the nucleus [4]. The types and amount of ECM can vary greatly between tissue types, and often change during tissue development and disease progression [1]. For example, fibronectin is the most abundant ECM component in fetal heart tissue. The proportion of fibronectin decreases during development and type I collagen becomes the most abundant ECM component in adult heart tissues [5]. Bone matrices are comprised primarily of a type I collagen matrix [6], but vary in calcium phosphate deposition [7]. Several bone dysplasias are caused by mutations in ECM components [8]. ECM composition also changes during disease progression such as cancer. Epithelial cancer has been shown to induce increases in collagen, fibronectin, elastin, and proteoglycans in ECM, as compared to healthy epithelial tissues [9].

Integrins are transmembrane receptors on cell membranes that support cell-ECM adhesion [10]. Integrins are heterodimers, composed of two subunits, α and β, and in mammals there are twenty-four α and nine β subunits that exist in various combinations [11]. Depending on the type of ECM, different integrin subunits are engaged to support cell adhesion [12]. Recent mechanotransduction studies have sought to investigate the role of different integrin subunits in various steps of in mechanotransduction [1]. Using fibronectin-coated beads and mouse embryonic fibroblasts, Roca-Cusachs, et al. showed α5β1-integrin determines adhesion strength, while αvβ3 is required for cells to sense the matrix stiffness and generate contractile forces [13]. A more recent study showed β1- and αv-class integrins cooperate to regulate myosin II during mechanosensing of kidney fibroblasts on fibronectin-coated substrates [14]. Most mechanotransduction studies have used type I collagen as the biochemical ligand to support cell adhesion. When cultured on collagen I-coated hydrogel substrates of varied stiffness, Engler, et al., showed aortic smooth muscle cells can change morphology [15] and Elosegui-Artola, et al., showed breast myoepithelial cells generate different amounts of traction force [16]. However, collagen-I does not bind to αvβ3 integrin, suggesting that other integrin subunits are involved in collagen-I mediated mechanotransduction. Together, these results suggest that the different integrin subunits engaged by different ECM types may have implications for the process of mechanotransduction, though this remains largely undemonstrated.

Polyacrylamide hydrogels have been widely used in previous mechanotransduction studies given their bioinert nature and ease for achieving tunable stiffness by changing the ratio of monomers. To support cell adhesion on polyacrylamide hydrogels, ECM proteins need to be chemically conjugated, often through the use of sulfo-SANPAH chemistry [17]. The most common used ECM proteins for supporting cell adhesion and for conjugation to polyacrylamide hydrogels include fibronectin [3,4,16,18–22], type I collagen [15,23–26], and laminin [19,27–29]. Type I collagen is the most abundant protein in the body, and can be found in most tissue types with varying densities. In contrast, type IV collagen and laminin are major constituents of basement membrane (BM), a specialized structure in epithelial and endothelial tissues [30]. Most detailed studies of YAP-mediated mechanotransduction have been conducted only with fibronectin [4,20,29,31]. It remains unknown how changing ECM type would impact mechanotransduction and YAP localization.

Using human mesenchymal stem cells (hMSCs) as a model cell type, the goal of this study was to assess the effects of varying ECM types and density on mechanotransduction and osteogenic differentiation of hMSCs. Cells were cultured on polyacrylamide hydrogels with tunable stiffness and biochemical ligands. In the present study, we chose two substrate stiffnesses (3 kPa and 38 kPa), which have been reported to induce adipogenesis and osteogenesis, respectively [26,32]. Our recent work also validate that this stiffness range was sufficient to induce differential responses in YAP translocation [33,34]. Four ECM types were compared including fibronectin, collagen-I, collagen-IV and laminin. We chose these ECM proteins based on their prevalence in native tissue ECM, common use for cell adhesion and with polyacrylamide hydrogels, and diversity in adhesive ligand sequences. We first sought to examine if YAP localization is dependent on ligand type. For each ECM type, we also varied the ligand density across a broad range (from 1 μg/ml to 100 μg/ml) to determine the optimal ligand density range that support stiffness-induced YAP translocation for each ECM type. To facilitate comparison, we chose a range of protein densities that cover a broad range used in previous studies [15,17,23,24,29,35,36]. To determine the types of integrin subunits required by each ECM type for mechanotransduction, hMSCs were incubated with antibodies blocking specific integrin subunits, and then cultured on hydrogels that were found to induce YAP nuclear localization without antibody blocking. Finally, the effects of varying ECM type on modulating osteogenesis were assessed by growing hMSCs on hydrogels coated with varying ECM types that support either cytoplasmic or nuclear YAP. Outcomes were analyzed by immunostaining of YAP, F-actin, and bone markers including RUNX2 and alkaline phosphatase (ALP).

2. Materials and methods

2.1. Hydrogel fabrication

Polyacrylamide hydrogels were fabricated by adapting a previously reported protocol [17,37] to incorporate primary amine end groups, for the purpose of enhancing protein conjugation efficiency. In brief, 2-aminoethyl methacrylate (Aldrich 516155, 15 mM in deionized water) was added to hydrogel precursor solution containing acrylamide (Sigma A4058, 40% (v/v)) and N,N′-methylenebisacrylamide (Sigma M1533, 2% (v/v)). Soft or stiff hydrogels were fabricated by maintaining acrylamide concentration constant (8% (v/v)) while varying the concentration of bis-acrylamide (0.08 or 0.48% (v/v)). To initiate photocrosslinking, photoinitiator 2-Hydroxy-1-[4-(2-hydroxyethoxy)phenyl]-2-methyl-1-propanone (Irgacure 2959, Ciba, 0.05% (w/v)) was used. Hydrogel precursor solution (65 μL) were loaded between two round glass coverslips (15 mm in diameter) and exposed to ultraviolet light (365 nm, 4 mW/cm2, 5 min) to form a hydrogel substrate with thickness of ~370 μm. The hydrogel surface was then modified with sulfo-SANPAH (Life Technologies 22589, 0.83 mg/ml in PBS) and exposed to light (365 nm, 4 mW/cm^2, 5 min). To incorporate biochemical ligand, hydrogel substrates were washed with PBS and incubated overnight at 37 °C in fibronectin (human, BD Biosciences 354008), type I collagen (rat tail, Corning CB40236), type IV collagen (from Engelbreth-Holm-Swarm murine sarcoma basement membrane, Sigma C0543), or laminin (from Engelbreth-Holm-Swarm murine sarcoma basement membrane, Sigma L2020) diluted in PBS at various densities.

2.2. Cell culture

Bone marrow-derived human mesenchymal stem cells (Lonza) were cultured in growth medium comprised of Dulbecco's Modified Eagle Medium (Gibco), fetal bovine serum (10% v/v, Gibco), penicillin-streptomycin (1% v/v, ThermoFisher Scientific), and recombinant human fibroblast growth factor-basic (10 ng/mL, Peprotech). For all studies, passage 6 hMSCs were

plated at 5000 cells/cm^2 onto the hydrogels, and cultured 6 h before analyzed by immunofluorescence staining. For osteogenic studies cells were seeded at 50,000 cells/ cm^2 and cultured for 5 days in osteogenic media comprised of DMEM, FBS (10%), penicillin/streptomycin (1% v/v, ThermoFisher Scientific), dexamethasone (100 nM), ascorbic-2-phosphate (50 μg/mL, Sigma), and beta glycerol phosphate (10 mM, Sigma).

2.3. Antibody blocking experiments

Integrin blocking experiments were conducted by incubating the cells in growth medium in the presence of αvβ3-integrin (25 μg/mL, Abcam ab78614), α5-integrin (25 μg/mL, Abcam ab78614), α2β1-integrin (25 μg/mL, Abcam ab24697), α1-integrin (25 μg/mL, Millipore MAB1973) for 1 h at 37 °C and then seeded onto the substrates with integrin antibody-containing medium and fixed after 5 h.

2.4. Immunofluorescence imaging

Cells were fixed using 4% paraformaldehyde/PBS for 15 min at room temperature, washed three times with washing buffer (0.1% Tween-20/PBS, 5 min), and permeabilized with 1% Triton X-100/PBS for 30 min. Samples were incubated in blocking buffer (3% BSA, 2% goat serum in PBS) for 30 min, then incubated with various primary antibodies including mouse anti-YAP (Santa Cruz Biotechnology, sc-101199), mouse anti-αvβ3-integrin (Abcam ab78614), mouse anti-β1-integrin (Abcam ab24693), rabbit anti-paxillin (Abcam ab32084), rabbit anti-pFAK (Abcam ab81298) overnight at 4 °C on a shaker. All antibodies were diluted in buffer at 1:100 except YAP antibody was diluted at 1:300. After washing, samples were incubated with corresponding secondary antibodies including Alexa 488 Goat-anti-mouse (Invitrogen A11001), rhodamine goat-anti-rabbit (Millipore AP132), rhodamine-phalloidin (Sigma P1951) for 1 h at room temperature on a shaker. All secondary antibodies were diluted at 1:300. Cell nucleus counter stain was performed using Hoeschst nuclear stain (Cell Signaling Technology 4082S, 2 μg/mL). Samples were washed with washing buffer (three times, 5 min per wash) before being imaged using a confocal microscope (10× air, 40× oil, or 100× oil immersion, Leica SP8 confocal system). To visualize protein coatings, substrates were washed with PBS and then immediately stained following the above protocol with blocking buffer, 1:100 primary antibody (anti-fibronectin in mouse, Sigma F0916; rabbit anti-collagen-I, Abcam ab34710; rabbit anti-collagen-IV Abcam ab6586; or rabbit anti-laminin, Abcam ab23753), and Alexa 488 Goat-anti-rabbit (Invitrogen A11034). All images were processed using open-source Fiji software [38,39]. Focal adhesions were characterized in hMSCs grown on stiff hydrogels coated with a ligand density found to support YAP translocation for each ECM type (10 μg/mL for fibronectin, 50 μg/mL for collagen-I, 20 μg/mL for collagen-IV, and 20 μg/mL for laminin).

2.5. Image analyses

To characterize YAP localization in a quantitative manner, we employed a method [21] which reports the ratio of nuclear YAP intensity vs. cytoplasm YAP intensity. In brief, a region of interest (ROI) in the nucleus and a region of interest of equal area in the cytoplasm immediately adjacent to the nucleus were selected. The nuclear region was defined using Hoechst staining. The fluorescence intensity of YAP staining within the nucleus ROI and the cytoplasm ROI were then quantified for an average of 35 (Fig. 2) to 45 (Fig. 4) cells per group in at least 2 independent experiments. Results are reported as the ratio of fluorescence intensity within nucleus vs. fluorescence intensity in cytoplasm. This same method was used to characterize RUNX2 localization and for this we used an average of 84 cells per group in at least 2 independent experiments (Fig. S7). To characterize the degree of F-actin polymerization in individual cells, images of phalloidin-stained cells were imported into Fiji software. The outer perimeter of the cell was selected as a region of interest (ROI) by thresholding the image and using the wand selection tool. The selection was then shrunk radially by 2 μm to define an inner perimeter. This allows us to calculate the integrated intensity within the inner region. The integrated intensity of the cortical region was calculated by subtracting the integrated intensity of the inner region from the integrated intensity from the total cell area. The final result was reported as the ratio between the integrated intensity within the inner region to the integrated intensity from the outer cortical region.

2.6. Western blot

To further characterize YAP localization, a nuclear and cytoplasmic extraction kit (Thermo Scientific) according was used to extract YAP following the manufacturer's instructions. Immediately following extraction, the protein was mixed with sample buffer (NuPAGE, Thermo Fisher Scientific) and TCEP. The protein was incubated at 75°F for 5 min and then loaded into a polyacrylamide gel (NuPAGE 4–12% Bis-Tris Protein Gels, Thermo Fisher Scientific). The gel was run at 200 V for 30 min in SDS MES running buffer, and then transferred to a membrane (Immobilon-P PDVF; EMD Millipore) at 20 V for 1 h in transfer buffer (NuPAGE, Thermo Fisher Scientific). Membranes were rinsed in water and incubated in 3% BSA, 2% goat serum blocking buffer for 2 h at room temperature. Membranes were then rinsed in Tris Buffered Saline solution with Tween 20 (TBST) and incubated in primary antibody for 1 h at room temperature (1:1000 YAP (D8H1X) XP, Cell Signaling Technology; 1:1000 Histone H3 (D1H2) XP, Cell Signaling Technology; 1:1000 HPRT, Abcam; 1:1000 Runx2, Cell Signaling Technology; 1:500 ALP, Abcam; 1:10,000 GAPDH, Cell Signaling Technology in SuperBlock T20, Thermo Fisher Scientific). Samples were washed 3 times, 5 min each in TBST, then incubated in secondary antibody (1:50,000 goat anti-rabbit HRP, Abcam in 3% BSA in TBS). After washing 3 times, 5 min each in TBST, membranes were rinsed in water and developed using SuperSignal West Femto Maximum Sensitivity Substrate (Thermo Fisher Scientific).

2.7. Gene expression

To further quantify the effect of varying ECM types on osteogenesis without changing substrate stiffness, RUNX2 localization was quantified, and quantitative RT-PCR was performed for RUNX2 and ALP after hMSCs were cultured for 3 days in osteogenic medium (Fig. S10). RNA was extracted using an RNeasy mini kit (Qiagen 74106). cDNA was synthesized using SuperScript III First-Strand Synthesis (Invitrogen 18080-051). qRT-PCR was performed following the manufacturer's protocol using Power SYBR Green PCR Master Mix (Life Technologies). All samples underwent 40 cycles on an Applied Biosystems 7900 Real-Time PCR System. The relative expression level of target genes was determined and plotted as 2^(−ddCt) values. Target gene expression was first normalized to an endogenous housekeeping gene (glyceraldehyde 3-phosphate dehydrogenase, GAPDH), followed by a second normalization to the expression level measured in day 0 control cells. The primers used are provided here in the 5′ to 3′ direction: GAPDH – ATGGGGAAGGTGAAGGTCG, GGGGTCATTGATGGCAACAATA; ALP – ACCACCACGAGAGTGAACCA, CGTTGTCTGAGTACCAGTCCC; RUNX2 – TGGTTACTGTCATGGCGGGTA, TCTCAGATCGTTGAACCTTGCTA.

2.8. Statistical analysis

Data are presented as mean ± standard deviations. For comparisons, data were analyzed with GraphPad Prism using one-way ANOVA by Tukey's multiple comparisons test or two-way ANOVA by Bonferroni's multiple comparisons test. Confidence intervals were kept at 95%, and P-values less than 0.05 were considered statistically significant.

3. Results

3.1. Characterization of hydrogels coated with varying types and densities of ECM proteins

Previous studies of YAP mechanotransduction have relied widely on fibronectin-coated hydrogel substrates. However, ECM is comprised of many other proteins that are known to have different effects on cell behavior. We fabricated soft (3 kPa) and stiff (38 kPa) polyacrylamide hydrogels coated with one of four ECM protein types: fibronectin, type I collagen, type IV collagen, and laminin (Fig. 1a). Hydrogels were coated with ECM solutions containing 1–100 μg/mL of ECM protein to test a range of coating densities covering what has been used in other studies. Immunohistochemistry for each specific ECM type revealed different ECM types exhibited different distributions and incorporation efficiencies on soft (Fig. 1b, c) and stiff (Fig. 1d, e) hydrogels. Fibronectin and laminin produced a more homogeneous distribution, whereas collagen-I and collagen-IV formed bundle-like structures on the hydrogel surface after coating. In addition to different distributions, different ECM protein types also exhibited different incorporation efficiencies, as shown by the fluorescence intensity. Among the four ECMs tested, fibronectin showed highest incorporation efficiency, and exhibited a higher incorporation efficiency on stiffer hydrogels (Fig. 1). Overall, the intensity increased with increasing density, though fibronectin and laminin incorporation peaked at 50 μg/mL and decreased at 100 μg/mL.

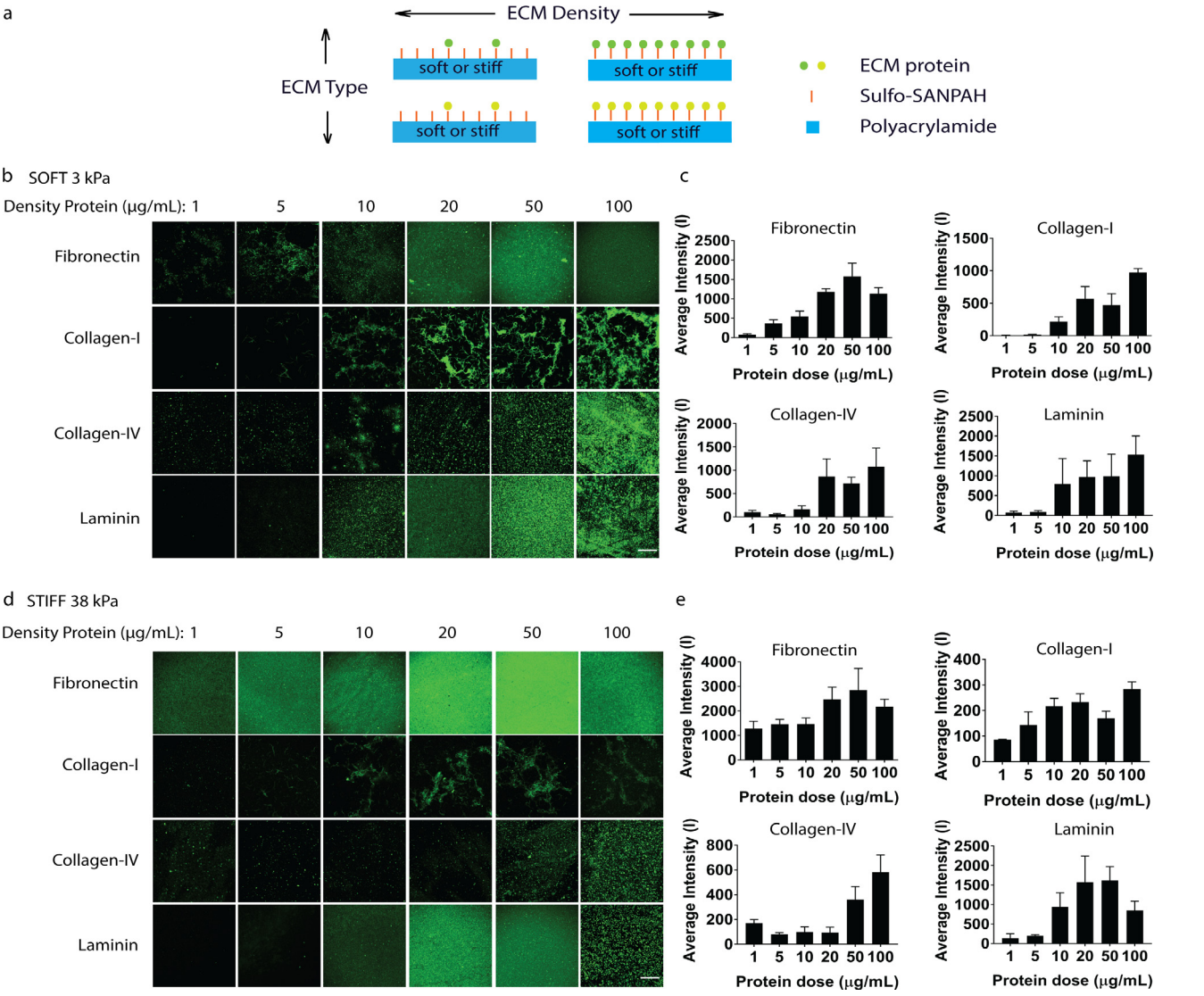

Fig. 1. Characterizing ECM protein incorporation with varying type on hydrogel substrates. (a) Schematic of experimental set up, (b) incorporation of various ECM proteins with tunable density on 3 kPa soft and (d) 38 kPa stiff hydrogels visualized with immunohistochemistry for the corresponding protein (first row, green: fibronectin; second row, green: collagen-I; third row, green: collagen-IV; fourth row, green: laminin) (Scale bars: 30 μm) and (c) quantification on 3 kPa soft and (e) 38 kPa stiff hydrogels of fluorescence intensity of immunohistochemistry staining of hydrogels coated with various doses of fibronectin (top left), collagen-I (top right), collagen-iv (bottom left), or laminin (bottom right). (For interpretation of the references to colour in this figure legend, the reader is referred to the web version of this article.)

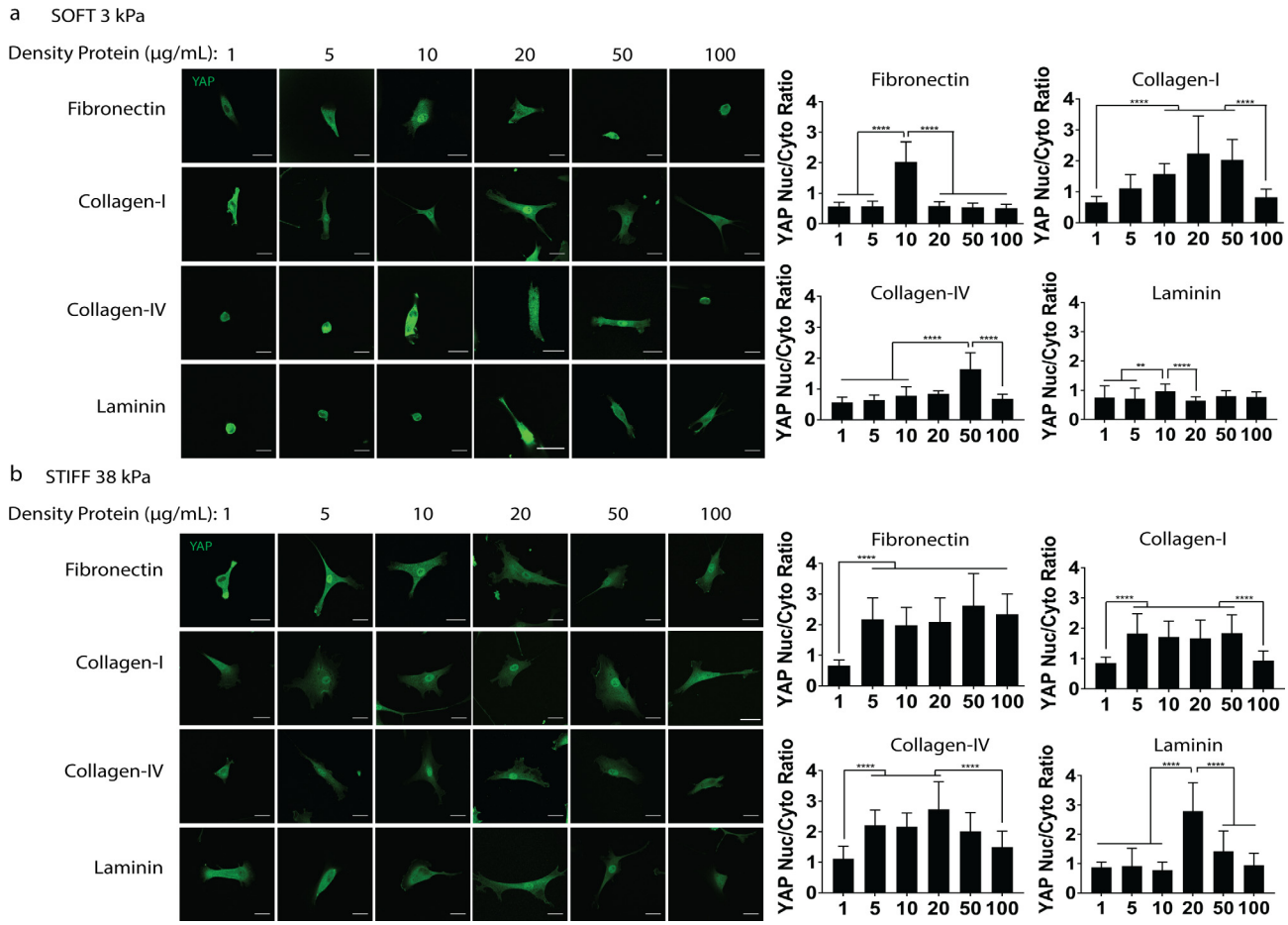

Fig. 2. YAP translocation depends on ligand type as well as density and stiffness. Effect of protein type on YAP translocation for hMSCs seeded on (a) soft and (b) stiff substrates with different ECM protein types and densities shown through individual cell images (green: YAP; Scale bar, 30 μm) and quantification of YAP localization. ****$p < 0.0001$. (For interpretation of the references to colour in this figure legend, the reader is referred to the web version of this article.)

3.2. ECM type modulates YAP translocation in a dose-dependent manner

We then assessed whether stiffness-induced YAP nuclear translocation also depends on ECM type. To minimize confounding factors from cell-secreted ECM, we fixed the cells 6 h after seeding for analyses. At low ECM density (1 μg/mL), both soft and stiff hydrogels led to cytoplasmic localization of YAP regardless of ECM type. Without changing hydrogel stiffness, increasing ECM density triggered nuclear YAP translocation, although the ligand density threshold required for such transition differs depending on ECM type (Fig. 2a, b). For example, when cultured on stiff hydrogels, YAP nuclear translocation occurs at low density (5 μg/mL) for fibronectin, collagen I and collagen IV, but required higher density (20 μg/mL) for laminin. Interestingly, on soft hydrogels, which has been reported to result in consistent cytoplasmic YAP localization in previous literature, increasing ligand density can induce nuclear YAP translocation using most of the tested ECM types. The only exception is laminin, with YAP remaining sequestered in the cytoplasm on soft hydrogels even at the highest density tested (100 μg/mL). Higher ligand density is also required for laminin to induce nuclear YAP translocation on stiff hydrogels as well—only 20–50 μg/mL of laminin on stiff hydrogels supported YAP translocation. We also provide these images at a higher magnification in the supporting information (Fig. S1). Regardless of substrate stiffness, increasing ligand density increased YAP nuclear translocation in a relatively biphasic relationship for collagen I and collagen IV. A similar trend was observed for fibronectin and laminin on stiff gels. In contrast, for fibronectin and laminin, YAP remained mostly cytoplasmic on soft hydrogels (Fig. S2). The trends observed in YAP localization correlated with F-actin cable formation (Fig. S3).

While the ligand density supporting nuclear translocation of YAP differs depending on ECM types, we report a ligand density for each ECM type that supports stiffness-induced YAP translocation (Fig. 3a, b). At this optimized ligand density, all ECM types supported increased cell spreading and F-actin cable formation in response to increasing hydrogel stiffness (Fig. 3a, b). We include larger versions of these images (Fig. S4) and lower magnification images to visualize cell attachment (Fig. S5) in the supporting information. In addition to immunostaining, YAP localization was also characterized by western blot following a procedure reported previously [40] (Fig. S6). The trend of western blot results is consistent with immunostaining (Fig. 3). For all ECM types, at the chosen optimal ligand density that supports stiffness-induced YAP translocation, higher nuclear YAP was observed on stiff hydrogel substrates, and higher cytoplasmic YAP was observed on soft hydrogel substrates.

3.3. Different ECM types engage different integrin subunits in YAP translocation

Next, we characterized focal adhesions expressed by hMSCs when cultured on hydrogels coated with different types of ECM proteins. For each ECM type, we chose a ligand density that induced strong YAP nuclear translocation on stiff substrates

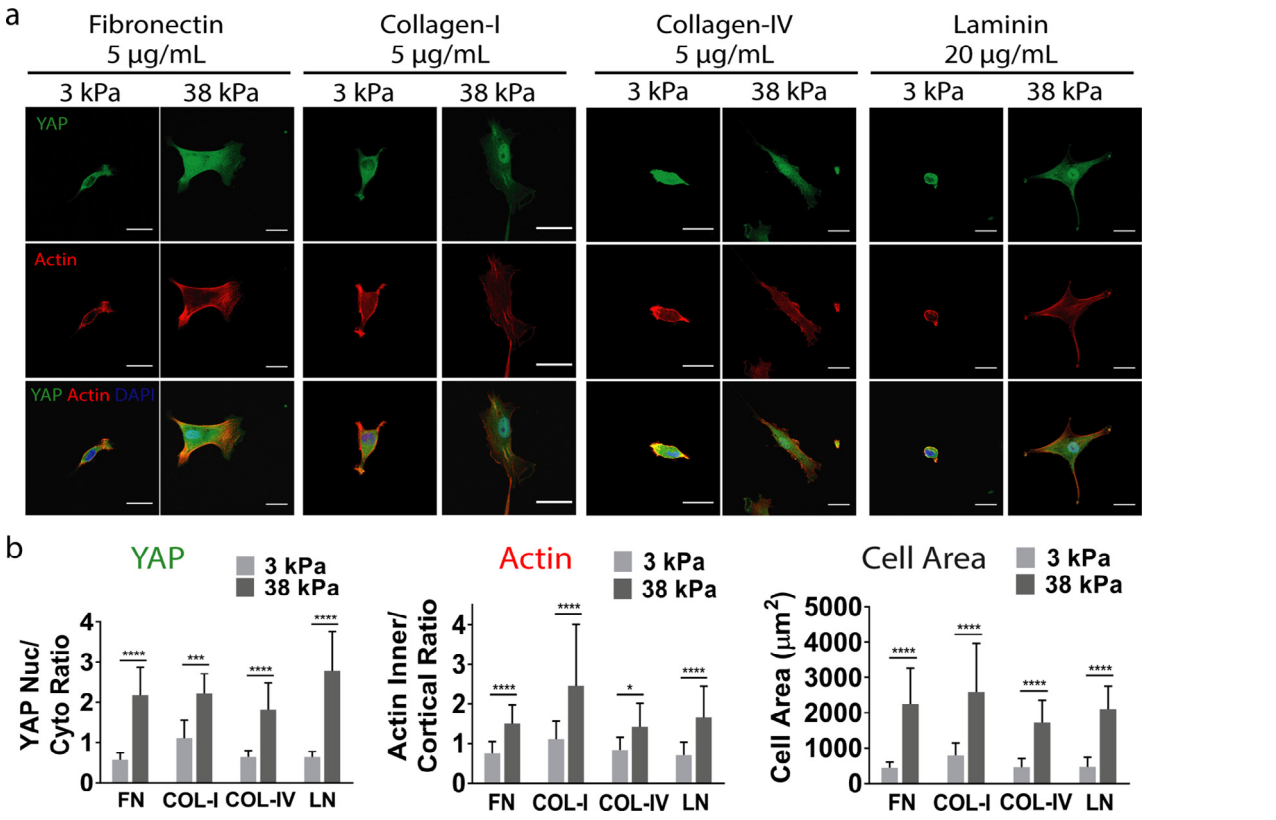

Fig. 3. Stiffness-dependent YAP translocation can be induced by all four ECM types, but each ECM requires a different optimized ligand density for this to occur. (a) Immunohistochemistry of hMSCs displaying conventional differences in YAP localization, F-actin formation, and cell spreading area with stiffness are observed for substrates coated with 5 μg/mL fibronectin, 5 μg/mL collagen-I, 5 μg/mL collagen-IV, and 20 μg/mL laminin (Scale bar: 30 μm) and (b) quantification of YAP localization, F-actin, and cell area. $^{****}p < 0.0001$.

(10 μg/mL for fibronectin, 50 μg/mL for type I collagen, 20 μg/mL for type IV collagen, and 20 μg/mL for laminin). Immunostaining confirmed focal adhesion formation with positive staining of pFAK, vinculin, and paxillin punctae (Fig. S7).

Using a functional assay, we blocked the adhesion of specific integrins and allowed them to adhere to stiff substrates coated with the various ECM protein types at these densities found to support strong YAP translocation (Fig. 4a, b). As expected, blocking adhesion of αvβ3-integrin, a fibronectin receptor [12], only inhibited YAP translocation on fibronectin. Interestingly, we observed that blocking adhesion of α5-integrin, another fibronectin receptor, inhibited YAP translocation not only on fibronectin but on all ECM protein types tested. Blocking adhesion of α1-integrin, a receptor for collagens and laminin, failed to inhibit YAP translocation on any ECM protein type. Blocking adhesion of α2β1-integrin, a subunit known to adhere to collagen and laminin proteins, inhibited YAP translocation on laminin and fibronectin coatings, while YAP remained nuclear on both type I and IV collagen. These results thus suggest that on different types of ECM protein, cells harness different integrin subunits to sense substrate stiffness and trigger YAP translocation (Fig. 4c).

3.4. Varying ECM type further modulates osteogenesis

As we have observed that YAP translocation is altered by varying ECM protein type and integrin interactions (Fig. 5a), we wanted to test the downstream effects on a pathway related to YAP translocation. We thus tested the effect of ECM protein type on osteogenesis. We cultured hMSCs in osteogenic medium on stiff substrates coated with two different densities of protein for each protein type—one that supported nuclear YAP translocation (Fig. 5b) and one that elicited cytoplasmic YAP sequestration (Fig. 5c) in short-term studies. Osteogenic differentiation was assessed by staining early osteogenic markers runt-related transcription factor 2 (RUNX2) and alkaline phosphatase (ALP) (Fig. 5b, c). At low ligand densities, while YAP localization was cytoplasmic for all ECM types, we observed low osteogenic commitment, as indicated by cytoplasmic RUNX2 and low ALP expression, for cells on hydrogels coated with collagen type I or fibronectin, consistent with the literature. However, some nuclear RUNX2 was observed on type IV collagen and laminin coated hydrogels. At high ligand densities leading to nuclear YAP localization, RUNX2 localization was nuclear, and higher levels of ALP were expressed on all ECM types except collagen type IV. Less RUNX2 and ALP expression was observed on type IV collagen-coated hydrogels. Quantification of RUNX2 location shows high density of FN, collagen I, and laminin coatings supported higher ratios of nuclear RUNX2, whereas collagen IV coating led to the lowest nuclear RUNX2 regardless of ligand densities (Fig. S8). To further characterize the effects of varying ECM type on modulating osteogenesis, western blot was performed for early bone markers ALP and RUNX2. Given the goal of the present study is to assess the effect of initial ECM coating on cell fates, it is important to limit the analyses to early time points only to avoid the confounding factors induced by new pericellular ECM deposited by MSCs. The trend of western blot results (Fig. S9) is consistent with the trend observed in immunostaining of RUNX2 and ALP staining (Fig. 5). For fibronectin and laminin, increasing bone marker expression was observed at high ligand density associated with YAP nuclear localization. A reverse trend was observed with Collagen IV, and no significant difference in bone markers was observed when Collagen I was used as the biochemical cue. Quantitative RT-PCR

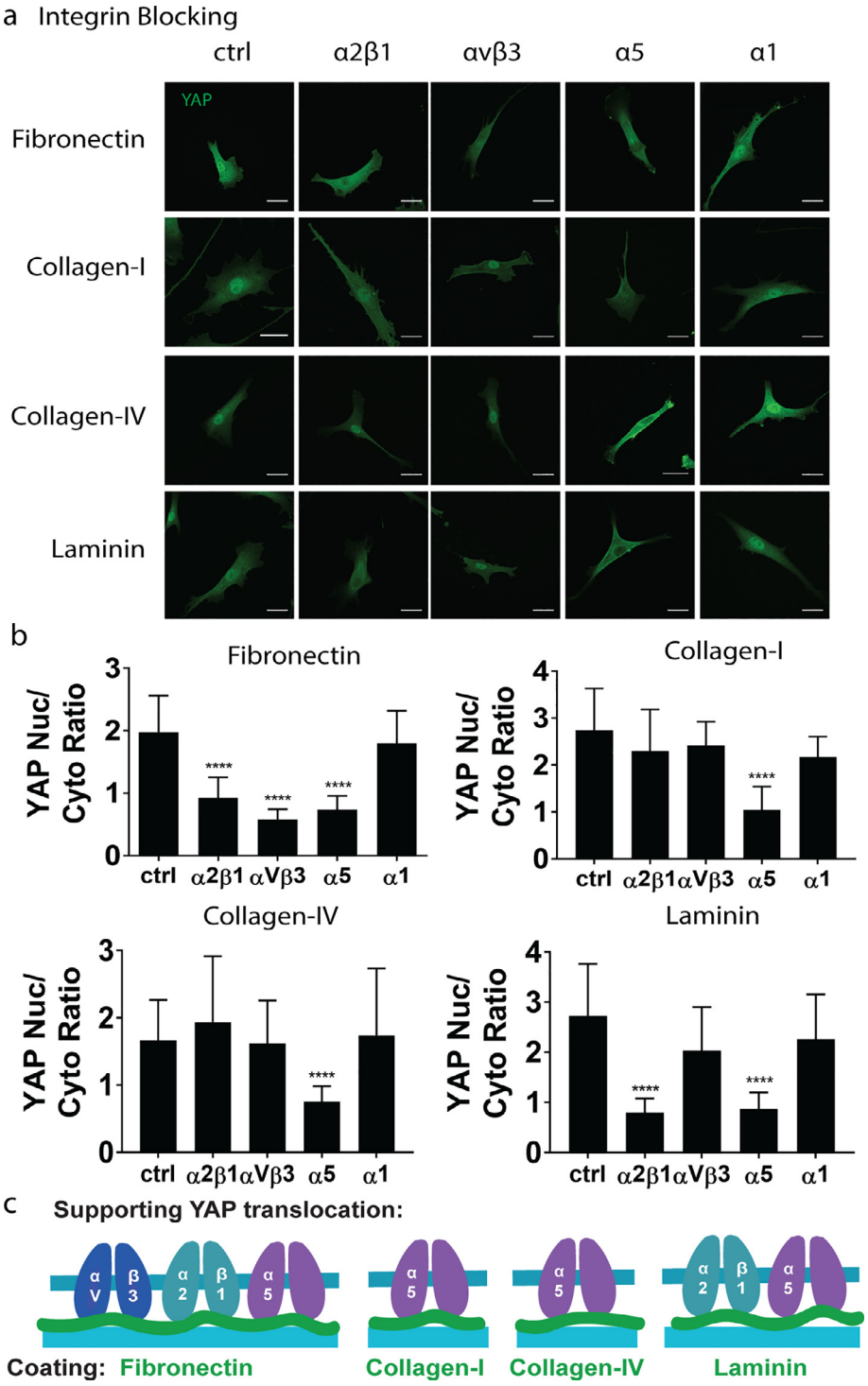

Fig. 4. Integrin subunit roles in YAP translocation depend on ECM type. (a) Immunostaining of YAP location in hMSCs when treated with antibodies blocking different integrin subunits. For each ECM type, hMSCs were cultured on stiff hydrogels coated with optimized ECM density that induce strong YAP nuclear translocation (10 μg/mL for fibronectin, 50 μg/mL for type I collagen, 20 μg/mL for type IV collagen, and 20 μg/mL for laminin) (green: YAP; Scale bar: 30 μm). (b) Quantification of YAP localization for each ECM type, $^{****}p < 0.0001$ and (c) summary schematic of the integrin subunits engaged by each of the ECM types tested in YAP translocation. (For interpretation of the references to colour in this figure legend, the reader is referred to the web version of this article.)

confirmed a similar trend for RUNX2, while high density of laminin led to the highest level of ALP expression among all groups (Fig. S10). These results indicate that ECM type further modulates osteogenic commitment of hMSCs.

4. Discussion

In the present study, we demonstrate that YAP translocation in hMSCs depends not only on substrate stiffness, but also on the ECM

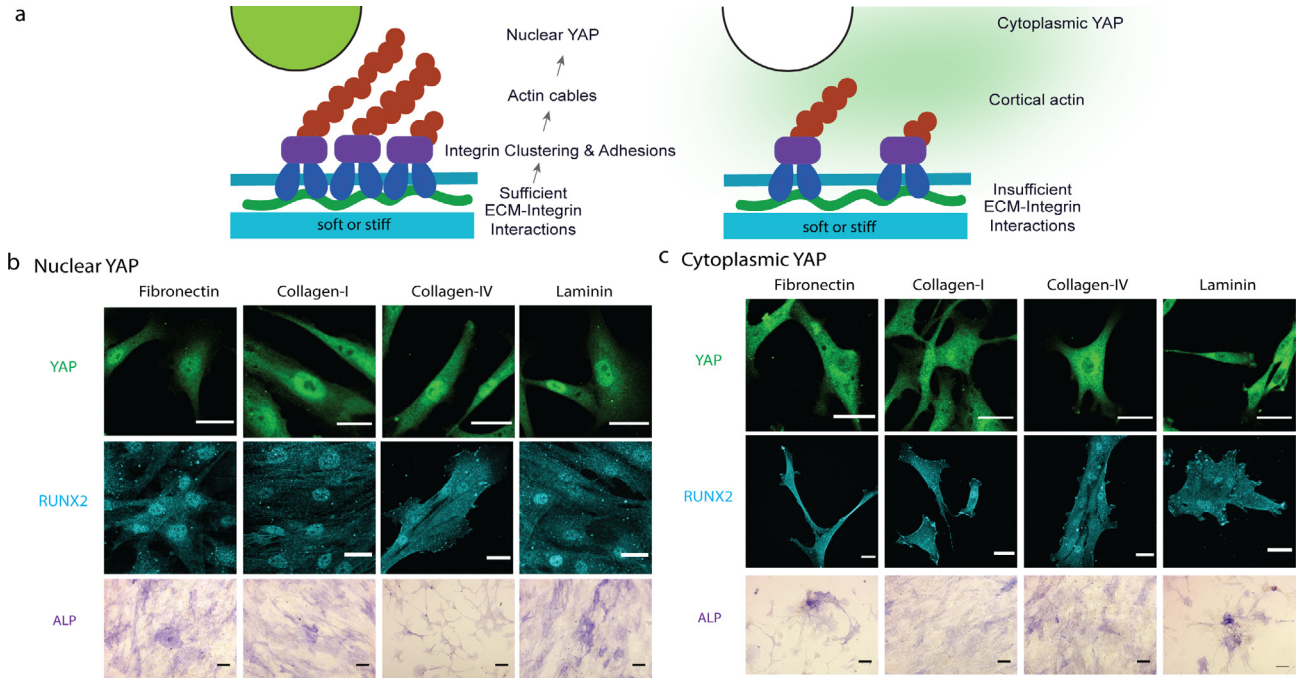

Fig. 5. Varying ECM type further modulates hMSC osteogenesis when cultured on stiff hydrogels that support either (b) nuclear YAP or (c) cytoplasmic YAP localization. Summary schematic illustrating (a) YAP localization is mediated through ECM-integrin interactions and actin assembly. For each ECM type, an optimized ligand density was chosen that supports the desired YAP localization. (b) High ligand densities were chosen for each ECM type that support nuclear YAP translocation (10 μg/mL for fibronectin, 50 μg/mL for collagen-I, 20 μg/mL for collagen-IV, and 20 μg/mL for laminin) and (c) a low ligand density (1 μg/mL) was chosen for all ECM types that leads to cytoplasmic YAP. Cells in all groups were cultured in osteogenic medium. Immunostaining of YAP localization was performed at 6 hr after to avoid confounding factor from cell-secreted ECM later (green: YAP; Scale bar: 30 μm); immunostaining of early bone markers, RUNX2 (Cyan) at day 3 and alkaline phosphatase (ALP, purple) at day 5. Scale bar: 30 μm for staining of YAP and RUNX2, 200 μm for ALP staining. (For interpretation of the references to colour in this figure legend, the reader is referred to the web version of this article.)

type used as biochemical ligands. We chose four major ECM types that are abundant in matrix, and have been widely used as coatings to support cell adhesion including fibronectin, type I collagen, type IV collagen, and laminin. The threshold range of ECM protein coating density to trigger nuclear YAP is ECM type- and substrate stiffness-dependent. We further demonstrate that YAP translocation requires different integrin subunits depending on the ECM type, and that altering ECM type further modulates osteogenic commitment independent of substrate stiffness.

Using fibronectin as the biochemical cue, one well established theory in the field of mechanotransduction is YAP localization is solely dependent on substrate stiffness, with soft substrates inducing cytoplasmic YAP, and stiff substrates inducing nuclear YAP. This trend was reproduced in our study as well, but it is only valid with a subset of fibronectin concentrations (5, 20, 50, and 100 μg/mL) (Fig. 2). Importantly, such stiffness-dependent YAP localization was no longer valid when hMSCs were cultured on hydrogels coated with certain fibronectin concentrations. Regardless of substrate stiffness, hydrogels coated with 1 μg/mL fibronectin consistently induced cytoplasmic YAP, whereas hydrogels coated with 10 μg/mL fibronectin supported nuclear YAP. The trend of YAP localization as a function of fibronectin density also varies with substrate stiffness. For soft hydrogels, peak YAP nuclear localization was observed at intermediate fibronectin density. In contrast, for stiff hydrogels, increasing fibronectin density led to increased YAP nuclear localization, which then plateaued. We also note that the ligand incorporation efficiency at a given ECM concentration varies on hydrogels with different stiffnesses (Fig. 1). This could be due to further differences in protein-surface interactions or porosity that could affect protein incorporation amount and distribution. We also observed a decrease in incorporation efficiency of fibronectin and laminin at higher densities, which was unexpected (Fig. 1). One possible interpretation for such a decrease is that when the protein concentration is increased beyond 50 μg/mL, more proteins bind to each other in the solution and form aggregates, decreasing the protein available for conjugation to the hydrogel substrate. These results suggest it is important to optimize protein concentration used for coatings to reach optimal conjugation efficiency.

For all four tested ECM types, varying ECM density can further modulate YAP translocation. However, the range of ligand density that leads to nuclear YAP differs across different ECM types. For example, when used in combination with soft substrates, type I collagen can induce YAP nuclear translocation for densities as low as 5 μg/ml, but type IV collagen required 50 μg/ml to induce YAP nuclear translocation. YAP translocation on collagen-I and collagen-IV is rather biphasic on both soft and stiff substrate substrates (Fig. 2). Interestingly, laminin was the only protein that maintained cytoplasmic YAP on soft substrates across all tested ligand density. Laminin only supported YAP nuclear translocation within a narrow range of ligand densities (20–50 μg/mL) on stiff substrates for the densities tested.

It is worth clarifying that different ligand densities were chosen for different experiments depending on the purpose of each experiment. The goal of Fig. 3 was to choose a ligand density that supports stiffness-dependent YAP localization. As such, we chose a ligand based on the dose-response curve for each ECM as shown in Fig. 2. Differently, we chose a ligand density that supports maximal nuclear YAP localization for each ECM type for other experiments (Fig. S6) (10 μg/mL for fibronectin, 50 μg/mL for type I collagen, 20 μg/mL for type IV collagen, and 20 μg/mL for laminin). The same ligand density was chosen for the integrin blocking experiments (Fig. 4) and the osteogenesis study (Fig. 5). We expect conditions with strong nuclear YAP localization to have strong

focal adhesion formation, consistent with previous literature by other groups [20] and our group [33]. Immunostaining confirmed focal adhesion formation with positive staining of pFAK, vinculin, and paxillin punctae at these densities (Fig. S7).

The observed impact on YAP localization in response to varying ECM types may be explained by several factors. First, different ECM types exhibit different incorporation efficiencies and distributions (Fig. 1) – differences that are inherent to each ECM type, for example, the availability of residues that can conjugate to the polyacrylamide surface. These differences could further influence mechanotransduction through changes in protein tethering and the availability of binding domains for integrin adhesion. Second, previous studies suggest that altering ECM type can change cell spreading [41], which is a cell fate that has been linked to mechanotransduction. Using fibronectin-coated substrates, previous studies have reported that increasing ligand density increases cell area [3,22,42]. In contrast, studies using type I collagen-coated substrates have reported a biphasic relationship with cell area reaching an optimum at intermediate ligand densities [15,43]. Furthermore, varying ECM type can also modulate cell traction forces in a differential manner. A study directly compared cell traction forces when cultured on hydrogels coated with similar concentration of type I collagen or fibronectin and showed fibronectin coatings induced higher traction forces than that of type I collagen for myoepithelial cells [16]. All of these factors may collectively contribute to the observed differences in YAP translocation in response to varying ECM types and density.

Cells sense matrix stiffness through cell adhesions and integrins play an important role in mechanotransduction. Our results fill an important gap of knowledge by identifying specific integrin subunits that are required to induce YAP translocation for different ECM types. While previous literature showed different ECM proteins require different integrin subunits for supporting cell adhesion, the role of integrin subunits in modulating YAP translocation remains unclear [12]. It has been suggested that αvβ3 may play a role in mechanotransduction [13]. Using fibronectin-coated hydrogels as a model system, our group recently reported that αvβ3-integrin is required for YAP nuclear translocation in hMSCs [33] for hMSCs on fibronectin-coated hydrogels. However, the role of integrin receptors in modulating YAP translocation for other ECM coatings remain largely unknown. To our knowledge, the present study is the first report that identifies specific integrin subunits that are involved in YAP translocation for different ECM types. In addition to αvβ3, we found that fibronectin-mediated mechanotransduction also requires α2β1- and α5-integrins, suggesting the cooperation of multiple integrin subunits. Unlike fibronectin, only α5-integrin was required for mediating YAP translocation using collagen I- and collagen IV-coated hydrogels. Interestingly, α5-integrin was found to be required for mediating YAP translocation in all four tested ECM types, an integrin that has previously been shown to mediate adhesive strength [13]. While it is known that α5-integrin adheres to the RGD domain of fibronectin [12], it has not been shown to adhere directly to collagen or laminin. Further work is needed to probe the mechanism involved, but α5-integrin is known to associate with other cell receptors, like integrin-associated protein CD47 [44] and the protein GIPC1 [45], which reportedly interacts with a number of different G-protein signaling and cytoskeleton-related proteins as well [46].

Mechanotransduction has been shown to play an important role in mediating stem cell differentiation. Using fibronectin-coated polyacrylamide hydrogels, recent studies in mechanotransduction have showed osteogenic differentiation of mesenchymal stem cells were enhanced with cell spreading and nuclear YAP localization [4]. ECM protein types have been shown to have differential effects on osteogenesis, with type I collagen [47] and laminin [48], for example, enhancing osteogenesis. Specific integrin subunits, such as α2, a subunit shown to adhere to collagen and laminin, have also been shown to upregulate osteogenic pathways [49]. However, the relationship between YAP translocation and osteogenesis for hMSCs adhered to different ECM types is largely unknown. Here we provided new evidence that even when hMSCs exhibit comparable levels of YAP localization, varying ECM protein type can directly impact osteogenesis. For example, when cultured on hydrogels that support nuclear YAP, fibronectin, collagen-I, and laminin induce much higher level of osteogenesis than collagen-IV, as shown by immunostaining of early bone markers RUNX2 and alkaline phosphatase (Fig. 5). In contrast, collagen-IV promotes osteogenesis when cells were exhibiting cytoplasmic YAP. Together, our results showed biochemical cues could be harnessed as a new parameter to synergize with mechanotransduction to promote desirable cell fates.

Future studies into the effects of other ECM proteins, as well as other ECM components, such as glycosaminoglycans, are of interest to further understand the cell niche. Combinations of different components and with different doses can also be used to understand combinatorial effects and to recapitulate complex niche environments. To better understand how varying ligand density and ECM types modulate mechanotransduction and cell fate, future studies can further characterize changes in protein tethering [23] and protein structural conformation [50], which have been shown to modulate cell fate. The interplay between cell-matrix and cell-cell interactions in this context is another interesting future direction. In this study we have intentionally chosen to use a low cell seeding density, so the observed changes are driven by cell-matrix interactions. It has been shown that cell-cell interactions can impact YAP localization [4] and the effect of varying cell density on mechanotransduction with substrates of varying ligand type could be tested.

The results from the present study provide a solid foundation for future work to further elucidate the role of ECM changes in normal tissue development or disease progression. For example, hydrogels with stiffnesses and ECM compositions that mimic different stages of cardiac tissue ECM during heart development [5] could enable mechanistic studies on how changes in these interactive niche cues drive heart development. Collagen-I matrices could also be incorporated with various concentrations of calcium phosphate to further probe changes in bone compositions during development or disease states on cell fate. Similar concepts could be used to model the cancer niche by mimicking the changes in ECM types and densities as well as tissue stiffnesses during cancer progression [9]. Since the parameters of such hydrogel platforms are well defined with cleaner compositions than in vivo tissues, they provide a more high-throughput platform for analyzing how changes in ECM cues modulate cell phenotype at various levels such as genetic, epigenetic, or proteomic differences.

5. Conclusions

In summary, the present study validates that the choice of ECM type directly modulates mechanotransduction of hMSCs, requires different integrin subunits, and can further modulate stem cell osteogenesis independent of substrate stiffness. These results highlight the necessity of considering biochemical ligand type and density in designing future mechanistic studies of mechanotransduction, as well as for optimizing choice of biochemical cues to promote stem cell differentiation and tissue regeneration. We demonstrate different ECM types exhibit varying degree of conjugation efficiency and distribution on hydrogels, which is likely due to inherent differences in the structures and properties ECM proteins. Future mechanistic studies could characterize the

physical properties of different ECM proteins to further elucidate the underlying mechanisms that explain the differences observed in this study. With over 300 proteins comprising the ECM [2] and at least 24 different integrin subunit combinations [12], this study provides a solid foundation and opens up doors for future work to assess other ECM proteins and the combinatorial effects of multiple ECM types. Together, such investigations will guide a more rational biomaterials design that can harness the cell-ECM interface to control cell fates both for promoting normal tissue development and for preventing disease progression.

Acknowledgements

The authors acknowledge NIH R01DE024772 (F.Y.), NSF CAREER award CBET-1351289 (F.Y.), California Institute for Regenerative Medicine Tools and Technologies Award RT3-07804 (F.Y.), the Stanford Bio-X Interdisciplinary Initiative Program (F.Y.), the Stanford Child Health Research Institute Faculty Scholar Award (F.Y.), the Bio-X Fellowship from the Stanford Bio-X Program (A.E.S.), and NIH T32GM008412 (A.E.S.) for support.

Appendix A. Supplementary data

Supplementary data to this article can be found online at https://doi.org/10.1016/j.actbio.2019.06.048.

References

[1] J.D. Humphrey, E.R. Dufresne, M.A. Schwartz, Mechanotransduction and extracellular matrix homeostasis, Nat. Rev. Mol. Cell Biol. 15 (2014) 802–812.
[2] R. Hynes, A. Naba, Overview of the matrisome–an inventory of extracellular matrix constituents and functions, Cold Spring Harb. Perspect. Biol. (2014).
[3] S.R. Peyton, A.J. Putnam, Extracellular matrix rigidity governs smooth muscle cell motility in a biphasic fashion, J. Cell Physiol. 204 (2005) 198–209.
[4] S. Dupont, L. Morsut, M. Aragona, E. Enzo, S. Giulitti, M. Cordenonsi, F. Zanconato, J. Le Digabel, M. Forcato, S. Bicciato, N. Elvassore, S. Piccolo, Role of YAP/TAZ in mechanotransduction, Nature 474 (2011) 179–183.
[5] C. Williams, K.P. Quinn, I. Georgakoudi, L.D. Black III, Young developmental age cardiac extracellular matrix promotes the expansion of neonatal cardiomyocytes in vitro, Acta Biomater. 10 (2014) 1–21.
[6] J. Rossert, B. de Crombrugghe, Type I collagen: structure, synthesis, and regulation, in Principles of Bone Biology, in: J.P. Bilezikian, L.G. Raisz, G.A. Rodan (Eds.), Principles of Bone Biology, Academic Press, San Diego, 2002, pp. 127–142.
[7] F.M. Watt, W.T.S. Huck, Role of the extracellular matrix in regulating stem cell fate, Nat. Rev. Mol. Cell Biol. 14 (2013) 467–473.
[8] J. Myllyharju, Extracellular matrix and developing growth plate, Curr. Osteoporos. Rep. 12 (2014) 439–445.
[9] C. Frantz, K.M. Stewart, V.M. Weaver, The extracellular matrix at a glance, J. Cell Sci. 123 (2010) 4195–4200.
[10] R.O. Hynes, Integrins: bidirectional, allosteric signaling machines, Cell 110 (2002) 673–687.
[11] B. Alberts, A. Johnson, J. Lewis, M. Raff, K. Roberts, P. Walter, Molecular Biology of the Cell, Garland Science, New York, 2002.
[12] J.D. Humphries, A. Byron, M.J. Humphries, Integrin ligands at a glance, J. Cell Sci. (2006) 3901–3903.
[13] P. Roca-Cusachs, N.C. Gauthier, A. del Rio, M.P. Sheetz, Clustering of alpha (5)beta(1) integrins determines adhesion strength whereas alpha(v)beta(3) and talin enable mechanotransduction, PNAS 106 (2009) 16245–16250.
[14] H.B. Schiller, M. Hermann, J. Polleux, T. Vignaud, S. Zanivan, C.C. Friedel, Z. Sun, A. Raducanu, K.E. Gottschalk, M. Thery, M. Mann, R. Faessler, b1- and av-class integrins cooperate to regulate myosin II during rigidity sensing of fibronectin-based microenvironments, Nat. Cell Biol. 15 (2013) 625–636.
[15] A. Engler, L. Bacakova, C. Newman, A. Hategan, M. Griffin, D. Discher, Substrate compliance versus ligand density in cell on gel responses, Biophys. J. 86 (2004) 617–628.
[16] A. Elosegui-Artola, E. Bazellieres, M.D. Allen, I. Andreu, R. Oria, R. Sunyer, J.J. Gomm, J.F. Marshall, J.L. Jones, X. Trepat, P. Roca-Cusachs, Rigidity sensing and adaptation through regulation of integrin types, Nat. Mater. 13 (2014) 631–637.
[17] R. Tse, A.J. Engler, Preparation of hydrogel substrates with tunable mechanical properties, Curr. Protoc. Cell Biol. 10 (2010) 1–16.
[18] W.J. Hadden, J.L. Young, A. Holle, M.L. McFetridge, D.Y. Kim, P. Wijesinghe, H. Taylor-Weiner, J.H. Wen, A.R. Lee, K. Bieback, B. Vo, D.D. Sampson, B.F. Kennedy, J.P. Spatz, A.J. Engler, Y.S. Choi, Stem cell migration and mechanotransduction on linear stiffness gradient hydrogels, PNAS 114 (2017) 5647–5652.
[19] C.D. Hartman, B.C. Isenberg, S.G. Chua, J.Y. Wong, Extracellular matrix type modulates cell migration on mechanical gradients, Exp. Cell Res. 359 (2017) 361–366.
[20] G. Nardone, J. Oliver-De La Cruz, J. Vrbsky, C. Martini, J. Pribyl, P. Skladal, M. Pesl, G. Caluori, S. Pagliari, F. Martino, Z. Maceckova, M. Hajduch, A. Sanz-Garcia, N.M. Pugno, G.B. Stokin, G. Forte, YAP regulates cell mechanics by controlling focal adhesion assembly, Nat. Commun. 8 (2017) 1–13.
[21] A. Elosegui-Artola, R. Oria, Y. Chen, A. Kosmalska, C. Perez-Gonzalez, N. Castro, C. Zhu, X. Trepat, P. Roca-Cusachs, Mechanical regulation of a molecular clutch defines force transmission and transduction in response to matrix rigidity, Nat. Cell Biol. 18 (2016) 540–548.
[22] A.D. Rape, M. Zibinsky, N. Murthy, S. Kumar, A synthetic hydrogel for the high-throughput study of cell-ECM interactions, Nat. Commun. 6 (2015).
[23] B. Trappmann, J.E. Gautrot, J.T. Connelly, D.G.T. Strange, Y. Li, M.L. Oyen, M.A. Cohen Stuart, H. Boehm, B. Li, V. Vogel, J.P. Spatz, F.M. Watt, W.T.S. Huck, Extracellular-matrix tethering regulates stem-cell fate, Nat. Mater. 11 (2012) 642–649.
[24] J.H. Wen, L.G. Vincent, A. Fuhrmann, Y.S. Choi, K.C. Hribar, H. Taylor-Weiner, S. Chen, A.J. Engler, Interplay of matrix stiffness and protein tethering in stem cell differentiation, Nat. Mater. 13 (2014) 979–987.
[25] L. Valon, A. Marin-Llaurado, T. Wyatt, G. Charras, X. Trepat, Optogenetic control of cellular forces and mechanotransduction, Nat. Commun. 8 (2017) 1–10.
[26] A.J. Engler, S. Sen, H.L. Sweeney, D.E. Discher, Matrix elasticity directs stem cell lineage specification, Cell 126 (2006) 677–689.
[27] J. Lee, A.A. Abdeen, X. Tang, T.A. Saif, K.A. Kilian, Matrix directed adipogenesis and neurogenesis of mesenchymal stem cells derived from adipose tissue and bone marrow, Acta Biomater. 42 (2016) 46–55.
[28] P.M. Gilbert, K.L. Havenstrite, K.E.G. Magnusson, A. Sacco, N.A. Leonardi, P. Kraft, N.K. Nguyen, S. Thrun, M.P. Lutolf, H.M. Blau, Substrate elasticity regulates skeletal muscle stem cell self-renewal in culture, Science 329 (2010) 1078–1081.
[29] A. Elosegui-Artola, I. Andreu, A.E.M. Beedle, A. Lezamiz, M. Uroz, A.J. Kosmalska, R. Oria, J.Z. Kechagia, P. Rico-Lastres, A. Le Roux, C.M. Shanahan, X. Trepat, D. Navajas, S. Garcia-Manyes, P. Roca-Cusachs, Force triggers YAP nuclear entry by regulating transport across nuclear pores, Cell 171 (2017) 1397–1410.
[30] V.S. LeBleu, B. MacDonald, R. Kalluri, Structure and function of basement membranes, Exp. Biol. Med. 232 (2007) 1121–1129.
[31] J. Shiu, L. Aires, Z. Lin, V. Vogel, Nanopillar force measurements reveal actin-cap-mediated YAP mechanotransduction, Nat. Cell Biol. 20 (2018) 262–271.
[32] R. McBeath, D.M. Pirone, C.M. Nelson, K. Bhadriraju, C.S. Chen, Cell shape, cytoskeletal tension, and RhoA regulate stem cell lineage commitment, Dev. Cell. 6 (2004) 483–495.
[33] A.E. Stanton, X. Tong, S. Lee, F. Yang, Biochemical ligand density regulates yes-associated protein translocation in stem cells through cytoskeletal tension and integrins, ACS Appl. Mater. Interfaces 11 (2019) 8849–8857.
[34] S. Lee, A.E. Stanton, X. Tong, F. Yang, Hydrogels with enhanced protein conjugation efficiency reveal stiffness-induced YAP localization in stem cells depends on biochemical cues, Biomaterials 202 (2019) 26–34.
[35] P.M. Rajagopalan, W.A. Marganski, X.Q. Brown, J.Y. Wong, Direct comparison of the spread area, contractility, and migration of balb/c 3T3 fibroblasts adhered to fibronectin- and RGD-modified substrata, Biophys. J. 87 (2004) 2818–2827.
[36] C.M. Williams, A.J. Engler, R.D. Slone, L.L. Galante, J.E. Schwarzbauer, Fibronectin expression modulates mammary epithelial cell proliferation during acinar differentiation, Cancer Res. 68 (2008) 3185–3192.
[37] R.J. Pelham, Y. Wang, Cell locomotion and focal adhesions are regulated by substrate flexibility, PNAS 94 (1997) 13661–13665.
[38] J. Schindelin, I. Arganda-Carreras, E. Frise, V. Kaynig, M. Longair, T. Pietzsch, S. Preibisch, C. Rueden, S. Saalfeld, B. Schmid, J.Y. Tinevez, D.J. White, V. Hartenstein, K. Eliceiri, P. Tomancak, A. Cardona, Fiji: an open-source platform for biological-image analysis, Nat. Methods 9 (2012) 676–682.
[39] J. Schindelin, C.T. Rueden, M.C. Hiner, K.W. Eliceiri, The ImageJ ecosystem: an open platform for biomedical image analysis, Mol. Reprod. Dev. 82 (2015) 518–529.
[40] B. Sen, Z. Xie, G. Uzer, W.R. Thompson, M. Styner, X. Wu, J. Rubin, Intranuclear actin regulates osteogenesis, Stem Cells 33 (2015) 3065–3076.
[41] A.S. Rowlands, P.A. George, J.J. Cooper-White, Directing osteogenic and myogenic differentiation of MSCs: interplay of stiffness and adhesive ligand presentation, Am. J. Physiol. Cell Physiol. 295 (2008) C1037–C1044.
[42] J.P. Lee, E. Kassianidou, J.I. MacDonald, M.B. Francis, S. Kumar, N-terminal specific conjugation of extracellular matrix proteins to 2-pyridinecarboxaldehyde functionalized polyacrylamide hydrogels, Biomaterials 102 (2016) 268–276.
[43] C. Gaudet, W.A. Marganski, S. Kim, C.T. Brown, V. Gunderia, M. Dembo, J.Y. Wong, Influence of type I collagen surface density on fibroblast spreading, motility, and contractility, Biophys. J. 85 (2003) 3329–3335.
[44] M.L. Orazizadeh, H.S. Lee, B. Groenendijk, S.J.M. Sadler, M.O. Wright, F.P. Lindberg, D.M. Salter, CD47 associates with alpha 5 integrin and regulates responses of human articular chondrocytes to mechanical stimulation in an in vitro model, Arthritis Res. Ther. 10 (2008) 1–11.
[45] T.T. Tani, A.M. Mercurio, PDZ interaction sites in integrin alpha subunits, J. Biol. Chem. 276 (2001) 36535–36542.

[46] L. De Vries, X. Lou, G. Zhao, B. Zheng, M.G. Farquhar, GIPC, a PDZ domain containing protein, interacts specifically with the C terminus of RGS-GAIP, PNAS 95 (1998) 12340–12345.
[47] A.K. Kundu, A.J. Putnam, Vitronectin and collagen I differentially regulate osteogenesis in mesenchymal stem cells, Biochem. Biophys. Res. Commun. 347 (2006) 347–357.
[48] R.F. Klees, R.M. Salasznyk, S. Vandenberg, K. Bennett, G.E. Plopper, Laminin-5 activates extracellular matrix production and osteogenic gene focusing in human mesenchymal stem cells, Matrix Biol. 26 (2007) 106–114.
[49] G. Xiao, D. Wang, M.D. Benson, G. Karsenty, R.T. Franceschi, Role of the alpha2-integrin in osteoblast-specific gene expression and activation of the Osf2 transcription factor, J. Biol. Chem. 273 (1998) 32988–32994.
[50] J. Mauney, V. Volloch, Progression of human bone marrow stromal cells into both osteogenic and adipogenic lineages is differentially regulated by structural conformation of collagen I matrix via distinct signaling pathways, Matrix Biol. 28 (2009) 239–250.